



Open camera or QR reader and scan code to access this article and other resources online.

# Inhalation of SP-101 Followed by Inhaled Doxorubicin Results in Robust and Durable *hCFTRΔR* Transgene Expression in the Airways of Wild-Type and Cystic Fibrosis Ferrets

Katherine J.D.A. Excoffon,<sup>\*,†</sup> Mark D. Smith,<sup>†</sup> Lillian Falese, Robert Schulingkamp, Shen Lin, Madhu Mahankali, Poornima K.L. Narayan, Matthew R. Glatfelter, Maria P. Limberis, Eric Yuen, and Roland Kolbeck

*Spirovant Sciences, Inc, Philadelphia, Pennsylvania, USA.*

<sup>†</sup>Both authors had equal contributions.

Cystic fibrosis (CF) is a serious genetic disease caused by mutations in the CF transmembrane conductance regulator (CFTR) gene. Approved small molecule therapies benefit the majority of people with CF (pwCF), but unfortunately not all. Gene addition offers a mutation agnostic treatment option for all pwCF. SP-101 is an adeno-associated virus gene therapy vector (AAV2.5T) that has been optimized for efficient human airway cell transduction, and that contains a functional and regulated shortened human CFTR minigene (*hCFTRΔR*) with a small synthetic promoter/enhancer. To understand SP-101 airway distribution, activity, and the associated immune response, *in vivo* studies were performed in wild-type and CF ferrets. After single dose inhaled delivery of SP-101, followed by single dose inhaled doxorubicin (an AAV transduction augments) or saline, SP-101 vector genomes were detected throughout the respiratory tract. *hCFTRΔR* mRNA expression was highest in ferrets also receiving doxorubicin and persisted for the duration of the study (13 weeks). Pre-existing mucus in the CF ferrets did not present a barrier to effective transduction. Binding and neutralizing antibodies to the AAV2.5T capsid were observed regardless of doxorubicin exposure. Only a portion of ferrets exhibited a weak T-cell response to AAV2.5T and no T-cell response was seen against *hCFTRΔR*. These data strongly support the continued development of inhaled SP-101, followed by inhaled doxorubicin, for the treatment of CF.

**Keywords:** cystic fibrosis, adeno-associated virus, ferrets, gene therapy, AAV2.5T

## INTRODUCTION

Cystic fibrosis (CF) is an autosomal recessive genetic disease that is an ideal target for gene therapy.<sup>1</sup> CF is caused by mutations in the gene that encodes the CF transmembrane conductance regulator (CFTR).<sup>2-4</sup> More than 2,000 CFTR mutations have been reported, many of which cause CFTR dysfunction and are categorized into seven classes, including mutations that result in premature stop codons which produce no functional protein (Class I) and mutations that cause a lack of CFTR mRNA (Class VII).<sup>2</sup> The emergence of small molecule modulators has demonstrated the

therapeutic impact of restoring CFTR activity in people with CFTR protein dysfunctions.<sup>2,4-6</sup> However, these modulators require the presence of CFTR protein and people with Class I and/or VII CFTR mutations do not benefit from this treatment. Moreover, some pwCF either do not respond well or poorly tolerate modulators.<sup>2,4-6</sup> Therefore, the development of novel treatment options, such as mutation-agnostic gene therapy, is warranted.

While CF is a multiorgan disease, the morbidity and mortality associated with CF stems from the chronic and progressively worsening mucosal obstruction and infection of

\*Correspondence: Dr. Katherine J.D.A. Excoffon, Spirovant Sciences, Inc., 3675 Market St., Suite 900, Philadelphia, PA 19104, USA. E-mail: kexcoffon@spirovant.com

the lungs.<sup>2,3</sup> Conceptually, the lung is an ideal target for gene therapy, since the inhaled route of delivery can be used to target the cells of the large and small airways. Nonetheless, several gene therapy clinical trials have shown that effective gene transfer to the airways is challenging.<sup>1,7–9</sup> The lungs have evolved a sophisticated barrier to most viral vectors and innovative strategies are required to breach this barrier for effective gene therapy.

Adeno-associated virus (AAV) is a small, non-pathogenic, helper-dependent virus that has been successfully developed as a gene therapeutic and recently approved for the treatment of genetic diseases, such as Leber congenital amaurosis (Luxturna<sup>TM</sup>, AAV2, 2017), spinal muscular atrophy type I (Zolgensma<sup>TM</sup>, AAV9, 2019), hemophilia B (Hemgenix<sup>TM</sup>, AAV5, 2022), hemophilia A (Roctavian<sup>TM</sup>, AAV5, 2023), and Duchenne muscular dystrophy (Elevidys<sup>TM</sup>, AAVrh74, 2023). It is evident that AAV-based vectors hold great promise for the treatment of additional genetic diseases.

AAV2 was the first AAV-based gene therapeutic that was clinically evaluated for CF airway disease.<sup>10</sup> While AAV2 vector genomes were detected post-dose in the nose, maxillary sinus, and lungs of treated subjects in multiple clinical trials,<sup>11–17</sup> the lack of a therapeutic response was concluded to be a consequence of several AAV2-related limitations. First, since the CFTR gene is large (4.45 kb) and at the packaging limit for AAV (~4.7 kb), expression of CFTR relied on the intrinsic promoter activity of the mandatory 145 bp inverted terminal repeats.<sup>10</sup> Moreover, AAV2 was subsequently shown to have low tropism for the apical surface of human airway epithelia *in vitro* and *in vivo*.<sup>18,19</sup>

In an effort to overcome the complex airway barriers, a directed evolution approach was applied to a shuffled and mutagenized AAV capsid library containing AAV2 and AAV5 sequences. Iterative selection, after application of the library to the apical surface of primary human airway epithelia (HAE), yielded a unique AAV capsid that was a hybrid of AAV2 and AAV5 with a single point mutation resulting in an amino acid change that is present within all three viral protein (VP) subunits of the AAV capsid (VP1, VP2, VP3; A581T in the VP1 sequence).<sup>20,21</sup> To overcome the genomic packaging limitation of AAV, a functional and regulated shortened human CFTR minigene (*hCFTRΔR*)<sup>22–24</sup> together with a small synthetic promoter/enhancer<sup>25</sup> were used to generate SP-101.

To better understand the barriers that the apical surface of the airway epithelium uniquely presents to AAV vector binding, entry, transduction, and gene expression, early gene transfer studies showed that small molecules capable of cellular proteasomal inhibition enhanced AAV-mediated mRNA expression and CF correction in CF HAE.<sup>26–29</sup> In particular, doxorubicin has been shown to enhance gene, and consequently protein, expression for many different AAV serotypes in airway cells, as well as in other human and non-human tissues.<sup>28–34</sup> Doxorubicin has also been demonstrated to enhance the activity of SP-101, leading to

the correction of CF HAE in a mutation agnostic manner (link to companion *in vitro* paper).

Recently AAV2.5T was shown to be tropic in ferret airway.<sup>31,32</sup> The ferret possesses several characteristics that are similar to humans which makes them a relevant animal model to support the development of SP-101. These include 1) airway cytoarchitecture, 2) CFTR gene expression patterns, 3) bioelectric and pharmacologic properties of the CFTR chloride channel, and 4) similar biology of recombinant AAV transduction in airway epithelia compared to humans. Of importance, ferrets have a similar transduction efficiency, including AAV serotype-specific differences in transduction that are influenced by epithelial polarity (apical vs basolateral) *in vitro*, and augmentation of AAV transduction with doxorubicin is similar to HAE.<sup>31,32,35</sup> Moreover, the CF ferret model has been developed to recapitulate key aspects of CF disease in humans.<sup>36–40</sup>

The CF ferret model presents with lung disease characterized by excessive mucus obstructing the airways, impaired mucociliary clearance, defective submucosal glands secretions, and polymicrobial bacterial infections.<sup>36–40</sup> However, these CF characteristics also afford significant limitations in its use since the CF ferrets are extremely sensitive to lung infections early in life, present with severe gastrointestinal (GI) defects prior to and soon after birth, along with meconium ileus, and develop exocrine pancreatic disease. To circumvent the mortality due to these GI conditions, the G551D CF ferret model was developed. This model is responsive to the small molecule CFTR potentiator ivacaftor (VX-770), and VX-770 treatment of the jill during gestation and of the kits post-partum improves survival rates. Withdrawal of VX-770 results in a rapid decline of lung function and reversal to the CF GI and pancreatic disease phenotype.<sup>40</sup>

Taken together, the ferret is a relevant species to investigate the biodistribution, *hCFTRΔR* mRNA expression and immunogenicity of aerosolized SP-101 followed by doxorubicin.

## MATERIALS AND METHODS

### Ethics statement

Spirovant-sponsored animal research was conducted only after appropriate ethical consideration and scientific review, and where no *in vitro* alternatives were available. Spirovant-sponsored animal studies were conducted in animal housing facilities that are fully accredited by the Association for Assessment and Accreditation of Laboratory Animal Care (AAALAC) International, following established guidelines, protocols, and Institutional Animal Care and Use Committee-approved procedures.

### Ferrets

Male and female, approximately 4-month-old, wild-type (WT) ferrets were sourced from Marshall BioResources (USA). Male and female, 3–5-month-old, G551D CF ferrets were sourced from J. Engelhardt at the University of Iowa,

Department of Anatomy & Cell Biology. CF ferrets were weaned off VX-770 (ivacaftor) for at least 4 weeks prior to dosing with SP-101. Following withdrawal of ivacaftor, these CF ferrets exhibit a CF phenotype consisting of weight loss, and associated dietary sensitivity, pancreatic insufficiency, increased lung mucus burden, and a thin, unkempt coat.

### Test articles

The SP-101 administered to groups I, II, and III was produced by Catalent<sup>®</sup> Cell and Gene Therapy (Baltimore, MD). Briefly, human embryonic kidney 293 (HEK293) cells were grown in serum-free, suspension culture conditions and then triple plasmid transiently transfected with pHelper, encoding the adenoviral helper genes, pRepCap, encoding the AAV2 Rep and AAV2.5T Cap genes, and a plasmid encoding the *hCFTRΔR* gene within AAV2 inverted terminal repeats (ITRs). Following transfection, cells were harvested, lysed, treated with benzonase, and clarified using depth filtration. Material was concentrated and diafiltered using tangential flow filtration (TFF). Column chromatography was performed on the TFF material using an ÄKTA chromatography system prior to concentration via diafiltration. Titer was determined by droplet digital PCR (ddPCR).

The SP-101 for groups V and VI was generated at the Children's Hospital of Philadelphia Vector Core. SP-101 was produced by co-transfection of the same three plasmids into adherent HEK293 cells, and lysate was purified by two rounds of CsCl<sub>2</sub> ultracentrifugation. TaqMan quantitative reverse transcription polymerase chain reaction (RT-qPCR) was used to quantify the titer of the purified viral stocks, as previously described.<sup>41</sup> Comparable potency, as determined *in vitro* by *hCFTRΔR*-mediated short circuit currents (Ussing) in CF-HAE, was observed between the two vector sources (data not shown). Doxorubicin hydrochloride (Pfizer Inc; Pharmaceutical grade commercial product) was purchased from a clinical pharmacy. Control saline (0.9% NaCl, sterile) for inhalation (group I, doxorubicin control, and group C-IV) was purchased from a clinical pharmacy. Control AAV Buffer (group C-VII) was provided by the Children's Hospital of Philadelphia Vector Core.

### Ferret dosing

Test article [SP-101, doxorubicin, or saline/AAV buffer control(s)] was administered to conscious, freely breathing, ferrets via nose-only inhalation within a plenum chamber system designed by Lovelace Biomedical (Albuquerque, NM). Exposure atmospheres were generated via a vibrating mesh nebulizer (Aerogen Solo), and the aerosol mixed with clean, filtered, air at a fixed flow rate (flow rate determined by number of concurrent animal exposures and specific test article aerosol characteristics) which transitioned the exposure atmosphere to flow past nose-only exposure tubes. Exposure atmospheres were generated using system configurations ensuring the particle size distribution, determined

by the mass median aerodynamic diameter, were <5 μm for each test article. The particle size distribution of the aerosols was measured at the breathing zone of the animal using a Mercer-style cascade impactor (In-Tox Products, Moriarty, NM) operated at a flow rate of 2.000 ± 0.100 L/min.

Total aerosol concentration in test atmospheres (SP-101, doxorubicin, and saline) was determined during each exposure period by sampling the exposure atmosphere from one of the chamber ports at a nominal flow rate of 0.750 ± 0.100 L/min through a filter and performing gravimetric analysis of filter samples.

SP-101 aerosol concentration was determined via collection in midget bubblers (two in series, each containing AAV formulation buffer) from one of the chamber ports of the exposure chamber (0.750 ± 0.100 L/min) for the duration of the exposure period. The titer of SP-101 in the AAV formulation buffer sample was then determined using an *hCFTRΔR* specific qPCR method, and the average SP-101 aerosol concentration determined by extrapolation to the total exposure atmosphere volume passed through the collection device.

Doxorubicin aerosol concentration was determined via a specific UPLC-UV chemistry assay on the filter samples collected from the exposure port of the system, with an extrapolation made for the volume of aerosol passed through the filter for each collection.

The dose of SP-101 was reported as vector genomes per gram of lung tissue (vg/g). The dose of doxorubicin was reported as μg per gram lung tissue (μg/g). Doses were calculated using equation 1.

$$Dose \left( \frac{A}{g} \right) = \frac{AC \left( \frac{vg}{L} \right) \times RMV \left( \frac{L}{min} \right) \times DF \times T (min)}{LW} \quad \text{Equation (1)}$$

Where A is either vector genomes (SP-101) or μg (doxorubicin), g is gram lung tissue, AC is the average aerosol concentration in the exposure atmosphere (vg/L, SP-101, or μ [AC units are microgram per liter for doxorubicin]) RMV is the respiratory minute volume (L per minute) T is the exposure time (min), LW is the weight of the lung tissue (g), and DF is the deposition fraction and is assumed to be 10% for the pulmonary deposited dose (Tepper et al. 2016).

### Study design

The data contained herein are comprised from separate *in vivo* studies (Table 1). In each study, ferrets were exposed via inhalation to SP-101, normal saline, or AAV buffer, followed by doxorubicin HCl or saline, on Day 1 with necropsy either 2 or 13-weeks (90 days) post-dose (see Table 1 for details).

Animals in groups I and III received the highest feasible deposited dose level of SP-101 in the lungs achievable

**Table 1.** Ferret Group Allocation, Dose Level and Tissue Sample Counts

Group ID	N per Group (Necropsy wk)	Genotype	SP-101 Deposited Lung Dose vg/g (lung weight)	Doxorubicin Deposited Lung Dose µg/g (Lung Weight)	Respiratory Tissue Sample Counts per Animal
I	20 (wk 2: 6M / 6F) (wk 13: 4M / 4F)	WT	9.6E11 (++)	saline (-)	Lung 2 Bronchus 2 Trachea 2 Nose 1
II	20 (wk 2: 6M / 6F) (wk 13: 4M / 4F)	WT	2.4E11 (+)	1.7 (+)	Lung 2 Bronchus 2 Trachea 2 Nose 1
III	20 (wk 2: 6M / 6F) (wk 13: 4M / 4F)	WT	1.0E12 (++)	1.8 (+)	Lung 2 Bronchus 2 Trachea 2 Nose 1
C-IV (control)	20 (wk 2: 6M / 6F) (wk 13: 4M / 4F)	WT	saline (-)	saline (-)	Lung 2 Bronchus 2 Trachea 2 Nose 1
V	3 (wk 2: 1M / 2F)	WT	1.3E11 (+)	9 (+)	Lung 2 Bronchus 4
VI	4 (wk 2: 1M / 3F)	CF <sup>a</sup>	2.6E11 (+)	9 (+)	Lung 2 Bronchus 4
C-VII (control)	7 WT: (wk 2: 2M / 1F) CF: (wk 2: 1M / 3F)	WT & CF <sup>a</sup>	AAV buffer (-)	saline (-)	Lung 2 Bronchus 4

<sup>a</sup>CF genotype: G551D homozygous.

wk, week; M, male; F, female; WT, wild-type; CF, cystic fibrosis.

within the constraints of this study design (group means of 9.6E11 to 1.1E12 vg/g lung tissue), whereas animals in groups II, V, and VI received a lower deposited dose of SP-101 (group means ranging from 1.3E11 to 2.6E11 vg/g lung weight). Group C-IV consisted of control animals that received an inhaled dose of normal saline for the same duration of time as the delivery of the higher dose of SP-101 in groups I and III. Group C-VII consisted of control WT and CF ferrets that received an inhaled dose of AAV formulation buffer for the same duration of time as the animals in groups V and VI. Doxorubicin HCl inhalation commenced either 2 h (groups II and III) or 4 h (groups V and VI), after completion of the SP-101 inhalation. The 2 or 4 h intervening period was based on the ability to complete all doses within a 24 h period. Lung deposited dose levels of doxorubicin were 1.7 or 1.8 µg/g (groups II and III respectively), or 9 µg/g lung weight (groups V and VI). Groups I (SP-101 only) and C-IV (control) received an inhalation exposure to normal saline 2 h after their previous exposure, to align with the doxorubicin exposures to groups II and III. These studies complied with all applicable sections of the Final Rules of the Animal Welfare Act regulations (9 CFR Parts 1, 2, and 3), as well as the Guide for the Care and Use of Laboratory Animals (2011), in a laboratory fully accredited by the AAALAC, Lovelace Biomedical, Albuquerque NM.

### mRNA isolation and RT-qPCR

To determine mRNA expression in ferret airway tissue, total RNA was prepared from frozen samples collected at necropsy. Tissue was lysed/homogenized with TRI Reagent (Zymo Research, Irvine, CA) and a TissueLyser (Qiagen, USA). For groups I–C-VI, a KingFisher Flex supported high-throughput sample preparation. For groups V–C-VII, the Direct-zol-96 RNA Kit (Zymo Research) was used for RNA extraction.

For RT-qPCR analysis, a validated *hCFTRΔR* mRNA expression assay was developed in compliance with Standard Operating Procedures at the animal housing facility and is consistent with US Food and Drug Administration (FDA), Guidance for Industry: Gene Therapy Clinical Trials-Observing Subjects for Delayed Adverse Events to support analysis of samples derived from Good Laboratory Practice for Nonclinical Laboratory Studies (U.S. FDA 21 Code of Federal Regulations (CFR) Part 58). Careful evaluation of the DNase conditions were required to ensure removal of all vector genomes prior to *hCFTRΔR* mRNA quantitation. For all RNA isolates, AAV vector genome DNA was removed by TURBO DNase treatment (Invitrogen, Waltham MA, USA). After TURBO DNase treatment, target concentrations of 500 ng RNA per PCR reaction were prepared for a duplexed 1-step reaction with primers/probe specific to the *hCFTRΔR* transgene and ferret *CFTR* endogenous genes. Samples

were prepared and handled on an epMotion Liquid Handler (Eppendorf, Enfield, CT) for the RT-qPCR assay. PCR was performed on a BioRad CFX384 Touch instrument (BioRad, Hercules, CA). Standard curves and independently aliquoted quality controls on each plate were prepared by diluting plasmids encoding *hCFTRΔR* or *fCFTR* genes. Cycle threshold (Ct) values were back calculated and data are presented as copies per  $\mu\text{g}$  RNA. The method lower limit of quantitation (LLOQ) is 200 copies per  $\mu\text{g}$  RNA (groups I–IV) and 50 copies per  $\mu\text{g}$  RNA (groups V and VI).

### DNA isolation and vector genome quantitation

To quantitate SP-101 vector genomes in ferret airway tissue, total DNA was prepared from frozen samples collected at necropsy. Tissues were homogenized with a TissueLyser (Qiagen, USA) and total DNA extracted following MagMAX-96 DNA Multi-Sample Kit (Invitrogen, Waltham MA, USA) manufacturer recommendations. A target concentration of 500 ng DNA was prepared for the qPCR reaction with primers and probe specific to SP-101 for the detection of vector genomes. Thermocycling on the BioRad CFX384 Touch instrument occurred in 4 steps: a UNG incubation 50°C (2 min), followed by activation at 95°C (5 min), denaturation at 95°C (3 s), and annealing/extension at 60°C (30 s). Using the CFX Maestro software, Ct values were back-calculated to a SP-101 plasmid-derived standard curve allowing for DNA quantitation in unknown samples. Vector genome DNA is presented as copies per  $\mu\text{g}$  DNA. The method lower limit of quantitation (LLOQ) is 50 copies per  $\mu\text{g}$  DNA.

### Total antibody immunogenicity assay

For groups I–C-IV, serum samples from all ferrets were collected pre-dose and at 2, 6, 9, and 13 (terminal) weeks post-dose and were analyzed for antibodies to SP-101 (anti-AAV2.5T) via a semi-quantitative, direct capture Enzyme Linked Immunosorbent Assay (ELISA). Briefly, each well of a 96-well Immulon High Bind plate (Thermo Scientific Cat #3855) was coated in 0.5  $\mu\text{g}/\text{mL}$  AAV2.5T vector, and then blocked with 1.0% ovalbumin. Diluted positive control and unknown samples were diluted and added to the plate and incubated at room temperature, shaking at  $\sim 450$  rpm for 1 h. The plate was washed in PBST and Protein A/G HRP detection reagent was added to the plate and incubated for 1 h. Following a wash step, TMB was added to the plate for up to 15 min, then quenched using KPL stop solution. Colorimetric detection occurred on the Spectramax i3 at 450 nm. Samples that screen positive are serially diluted/tested and data presented as titer values, the dilution at which the sample crosses the assay positive/negative cut-off.

### Neutralizing antibody (NAb) immunogenicity assay

For groups I–C-IV, serum samples from ferrets taken pre-dose and at 2, 6, 9, and 13 (terminal) weeks post-dose were analyzed for AAV2.5T capsid-specific NAb using an in vitro HEK293-cell based assay, as previously described.<sup>42,43</sup> All samples were serially diluted and tested in the assay to determine a sample titer. Briefly, serum samples were heat inactivated at 56°C for 35 min, then incubated with recombinant AAV2.5T.CMV.LacZ (1E9 genomic copies/well) for 1 h at 37°C. The serum sample/reporter vector mixture was then added to the HEK293 cells, seeded at 1E5 cells on 96-well plates. After a 1 h incubation and cell lysis, the lysate was developed with the mammalian  $\beta$ -galactosidase assay kit, in accordance with the manufacturers' instructions (Applied Biosystems, Thermo Fisher Scientific). Detection occurred on a microplate luminometer (Clarity, BioTek). Those with signals below the assay cut point (positive cut-off) were considered positive for anti-AAV2.5T NAb. Data are presented as titers, the highest serum dilution at which AAV transduction is reduced 50% compared to a negative control. The lowest dilution investigated was a 1:5 sample dilution.

### IFN- $\gamma$ ELISpot

For groups I–C-IV, ferret PBMC were isolated from whole blood collected into BD Vacutainer<sup>®</sup> CPT<sup>™</sup> Cell Preparation Tubes (BD&Co., Franklin Lakes, NJ) with Sodium Heparin as the anticoagulant at necropsy. The PBMC isolation protocol followed manufacturer instructions with minor adjustments per animal housing facility SOPs. The PBMC pellet was resuspended in a 10% dimethylsulfoxide (DMSO)/fetal bovine serum (FBS) freezing medium to a concentration of  $1 \times 10^6$  cells/mL and transferred into a pre-chilled (4°C) freezing container and placed at  $-80^\circ\text{C}$  for at least 24 h prior to transfer to the vapor phase of the liquid N<sub>2</sub> freezer. Three overlapping peptide pools (15mers overlapping by 10 amino acids [aa]) of AAV2.5T capsid protein and 5 pools for the *hCFTRΔR* transgene product were custom synthesized with capping (to avoid any deletions) by JPT Peptide Technologies GmbH (Berlin, Germany). Each peptide pool spanned approximately 48–56 aa of the respective protein. The assay was adapted for PBMCs and performed as previously described.<sup>44</sup> Briefly, PBMCs were stimulated with one of the three AAV2.5T, or five *hCFTRΔR*, peptide pools and data were reported as spot forming units (SFU) per million PBMCs. The positive controls consisted of PBMCs stimulated with two different concentrations of phorbol myristate acetate plus ionomycin (PMA + ION). Negative controls were PBMCs in the presence of DMSO only. A sample was considered positive when the value was three times the value generated in the presence of DMSO (55 SFU per million PBMCs; cut-off value, established prior to sample analysis by screening the

mock responses in a set of PBMCs derived from untreated ferrets).

### BaseScope

Formalin-fixed paraffin embedded ferret tissue sections were cut into  $5 \pm 1 \mu\text{M}$  sections. A BaseScope 2ZZ probe targeting the sense strand of SP-101 was designed and was specific for SP-101 vector genomes only. Hybridization was performed at Advanced Cell Diagnostic according to the manufacturer's protocol. To ensure the specificity of the probe, sections were either untreated or treated with DNase at  $40^\circ\text{C}$  for 30 min. Then, a BA-hCFTRdR-2zz-st-sense-C1 probe, that targets the SP-101 vector genome, was added and allowed to hybridize at  $40^\circ\text{C}$  for 2H. Post-hybridization, the slides were washed in wash buffer and subjected to a series of BaseScope Amp steps that amplify signal. Fast red substrate was then added to the sections for 10 min at RT and the slides were counterstained with 50% hematoxylin. The slides were dried at  $60^\circ\text{C}$  and mounted using VectaMount. The next day the slides were evaluated using a standard bright field microscope under 40X magnification. Images were analyzed using Aperio ImageScope (v12.4.6.5003) software.

### Statistics

Statistical analyses were performed by Biodata Solutions using R software (version 4.3.0). A mixed model approach was fitted to the data for the following response variables:

- Figure 2: DNA (log-transformed)
- Figure 3: RNA (log-transformed)
- Figure 6B: DNA (log-transformed)
- Figure 6C: RNA (log-transformed)

In all models, "Animal ID" was treated as a random effect. For Figures 2 and 3, the fixed effects were "sex," "tissue," "collection timepoint," and "dose group." Fixed effects for Figure 6B and C were "tissue," "CF or WT."

Interactions between the fixed effects were evaluated for statistical significance: three-way for Figures 2 and 3, two-way for Figure 6B and C. However, a significant interaction was determined, fixed effects were then varied one at a time and evaluated via pair-wise comparisons.

A Benjamini–Hochberg procedure was implemented to adjust for multiplicity. This method effectively controls the False Discovery Rate (FDR) when conducting multiple hypothesis tests or comparisons and the FDR level of 5% is applied at the graph/model level, ensuring control over false positives for all hypotheses collectively.

Box plots represent the upper and lower quartile values (25–75% of data values). The median is represented by the midline and the whiskers extend to the 10th and 90th percentile of the data. Samples with levels less than the

LLOQ are plotted as 50 or 200 copies per  $\mu\text{g}/\text{DNA}$  or RNA, respectively.

## RESULTS

### Development of validated molecular assays

The methods for qPCR, for SP-101 vg, and RT-qPCR, for *hCFTRΔR* mRNA, assays, as well as RNA isolation followed by TURBO DNase treatment, prior to RT-qPCR, were validated for multiple parameters including SP-101 plasmid standard curve performance, accuracy and precision, selectivity, and sample stability. Figure 1 shows the optimization of the RT-qPCR method to confirm removal of vector genomes to accurately quantify *hCFTRΔR* mRNA. Total RNA was isolated from CF-human airway epithelia (HAE) transduced apically with SP-101 at an MOI of  $1\text{E}5$  with doxorubicin at  $1 \mu\text{M}$  in the basal media (reference accompanying article for details) and *hCFTRΔR* mRNA was quantified by RT-qPCR, with or without reverse transcriptase (RT), after treatment with TURBO DNase (Fig. 1A). Since RT converts all mRNA or single-stranded AAV vg into double-stranded cDNA before measurement by qPCR, these data demonstrate the requirement for effective removal of all vector genomes for the specific detection of *hCFTRΔR* mRNA. Red-dotted lines highlight *hCFTRΔR* mRNA copy counts resulting from the presence of SP-101 vector genomes which are present in the absence of TURBO DNase treatment. Following optimization of the assay conditions for CF HAE, bronchus tissue from ferrets exposed to an SP-101 deposited lung dose of  $2.8\text{e}11 \text{ vg/g}$  (tissues collected 3 days post dose), had RNA extracted and subjected to treatment by either DNase I contained in the RNA kit or TURBO DNase reagents. Vector genomes were not fully removed after DNase I treatment which resulted in inflated *hCFTRΔR* mRNA counts (Fig. 1B). Key validation parameters and performance data are presented in Figure 1C and D. As an additional measure of data integrity, endogenous *fCFTR* mRNA levels were also quantified to ensure the final TURBO DNase protocol did not affect the overall mRNA signal in the sample.

### SP-101 demonstrates broad biodistribution in ferret airways

WT ferrets were dosed, and samples taken as shown in Figure 2A. Biodistribution of SP-101 in the respiratory tract was assessed by qPCR for groups I, II, and III, at 2- and 13-weeks post-dose (Fig. 2B–E). Analysis of tissue samples from control animals (group C-IV) returned occasional samples greater than the lower level of quantitation (LLOQ; 5/96 on Day 14, 12/64 on Day 90), albeit at levels considerably lower than the treated groups (I–III). All of these control samples returned mRNA levels below the LLOQ, indicating a lack of exposure of these control animals

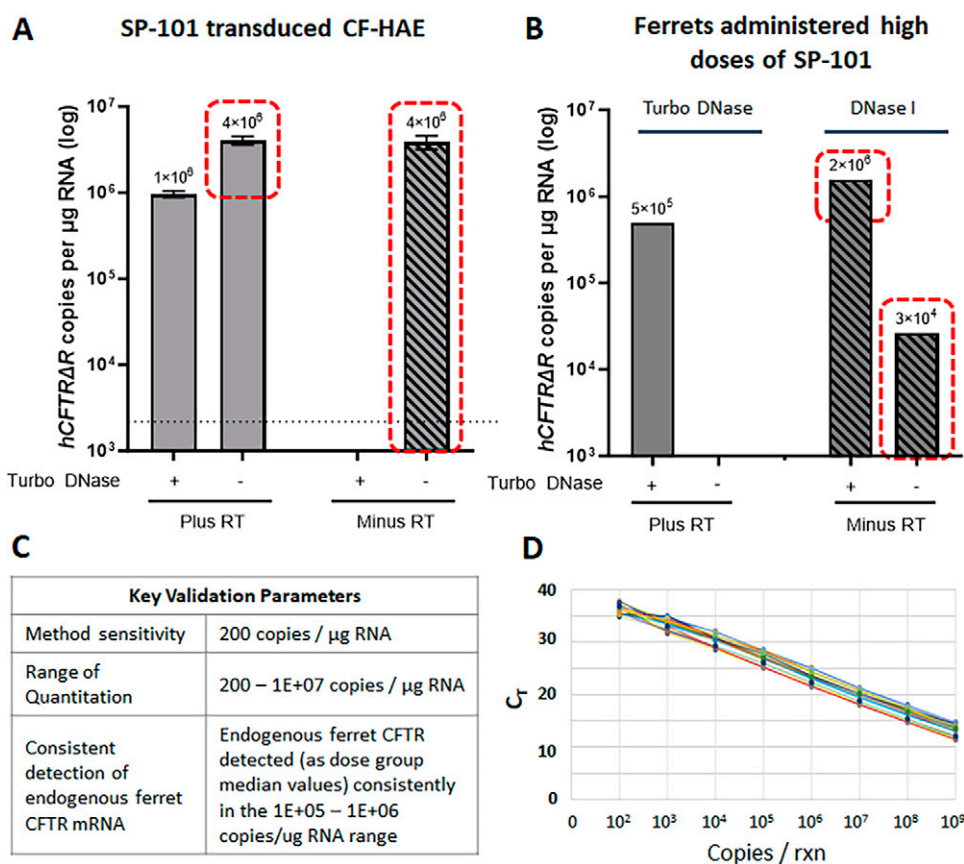


**Figure 1.** Validation of a *hCFTRΔR* mRNA copy detection method (RT-qPCR) in ferret tissue. Prior to validation, the RT-qPCR method was carefully optimized to confirm removal of vector genomes to accurately quantify *hCFTRΔR* mRNA in (A) CF HAE transduced apically with SP-101 at an MOI of  $1\text{E}5$  with doxorubicin at  $1 \mu\text{M}$  in the basal media or (B) bronchus tissue from ferrets exposed to an SP-101 deposited lung dose of  $2.8\text{E}11$  vg/g. *hCFTRΔR* mRNA was quantified by RT-qPCR, with or without reverse transcriptase (RT), after treatment with two commercially-available forms of DNase: TurboDNase or Dnase I. For A) and B), red dotted lines highlight *hCFTRΔR* counts resulting from the presence of SP-101 vector genomes. (C) Key parameters for the RT-qPCR method validation are shown. The method validation was conducted consistently with the FDA Guidance for Industry: Gene Therapy Clinical Trials—Observing Subjects for Delayed Adverse Events to support analysis of samples derived from Good Laboratory Practice for Nonclinical Laboratory Studies (U.S. FDA 21 CFR Part 58). Also evaluated were method precision and accuracy, selectivity and extract stability. (D) The range of quantitation was evaluated by preparing and testing a SP-101 plasmid standard curve during validation and sample analysis. CF, cystic fibrosis; HAE, human airway epithelia; rxn, reaction.

to infectious AAV (Fig. 3). SP-101 vg levels demonstrated both dose and regional differences. Groups I and III both received similar doses of SP-101 and had similar SP-101 vg levels at 2-weeks while group II received a lower dose with corresponding lower median levels of SP-101 vg/ $\mu\text{g}$  total DNA. By 2-weeks post dose, the highest deposition was observed in sections taken from parenchymal lung tissue while levels were lowest in the sections of tracheal tissue. By 13 weeks post-dose, SP-101 vg had declined by approximately 3-log compared to the 2-week levels indicating that much of the initial SP-101 dose had been cleared. Dosing with doxorubicin HCl did not appear to affect SP-101 vg/ $\mu\text{g}$  total DNA between groups I and III, except at 13 weeks in the lung and trachea which maybe the result of variable SP-101 clearance and tissue sampling.

SP-101 vg were also detected in numerous other tissues at week 2, although generally at lower levels than those observed in lung and bronchi (Supplementary Fig. S1A).

The non-respiratory organ with the highest SP-101 vg level was liver, with levels at least 10-fold lower than those of the lung. In these non-respiratory tissues, similar to respiratory tissues, SP-101 vg levels at 13 weeks were considerably lower than observed on week 2 (Supplementary Fig. S1B).

#### SP-101-mediated *hCFTRΔR* mRNA expression in ferret airways is increased by doxorubicin HCl and is durable

SP-101 transduction was evaluated for groups I, II, and III by measuring *hCFTRΔR* mRNA expression via RT-qPCR at 2- or 13-weeks post-dose (Fig. 3). Endogenous ferret CFTR (*fCFTR*) mRNA expression was also evaluated to assess the relationship between *fCFTR* mRNA expression in the dosed animals and the *hCFTRΔR* mRNA levels in each tissue (dotted lines). Analysis of tissues samples from control animals (group C-IV) returned values below the lower limit of quantitation. In contrast to no

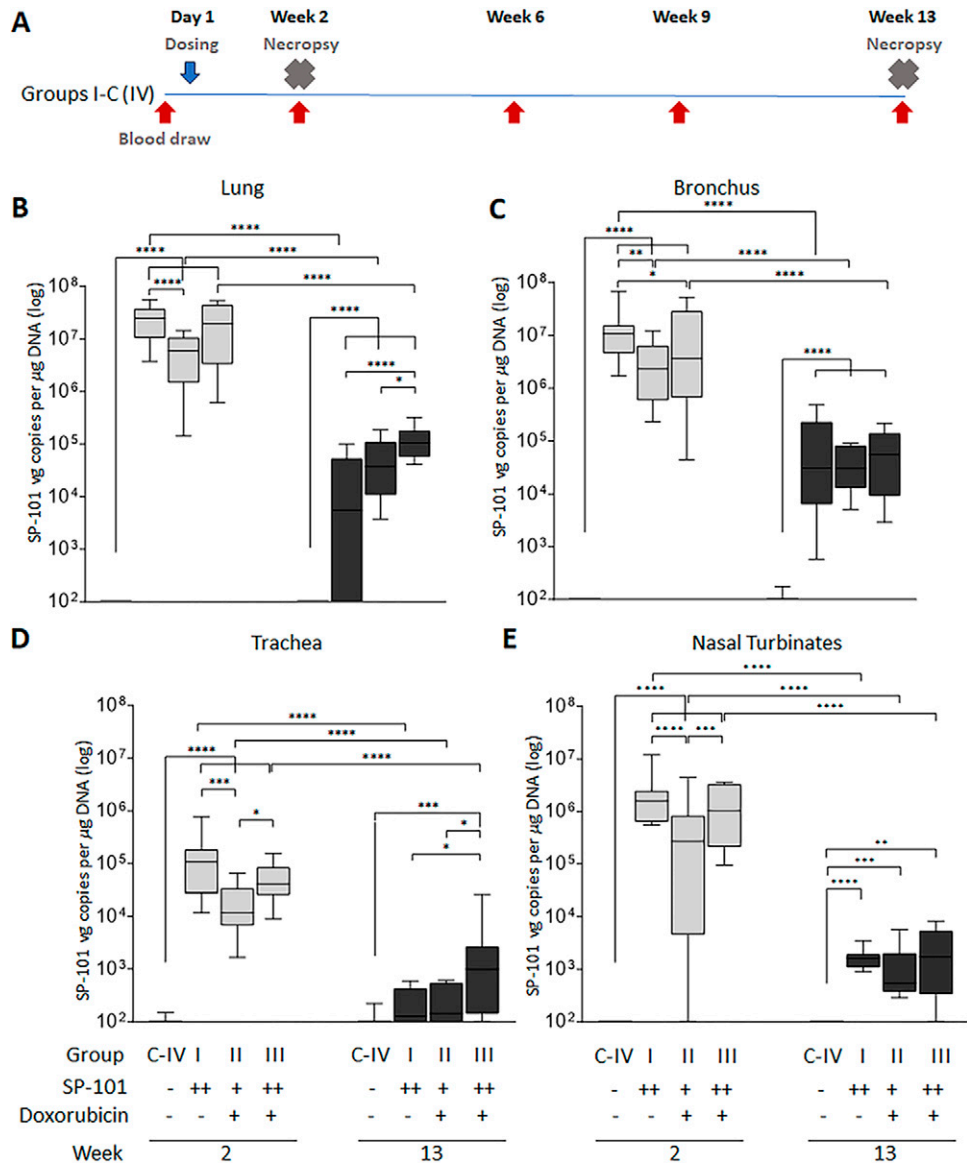


**Figure 2.** SP-101 vector genome (vg) copies are dose-responsive but do not change with doxorubicin administration. **(A)** Schematic of the study and sampling timeline. Target tissues from groups C-IV and I-III were collected 2- or 13-weeks post-dose and evaluated for SP-101 vg by qPCR in **(B)** lung, **(C)** bronchus, **(D)** trachea ( $n = 14\text{--}24$ ) or **(E)** nasal turbinates ( $n = 5\text{--}12$  tissue samples per group). ++ represents a high dose of SP-101 and + represents a low dose of SP-101. For doxorubicin, + or - represents with or without doxorubicin (Dox). Ct values were back-calculated to the standard curve and data are presented as SP-101 vg copies/ $\mu\text{g}$  DNA. The method lower limit of quantitation (LLOQ) is 50 copies per  $\mu\text{g}$  DNA. Samples with levels less than the LLOQ are plotted as 50 copies/ $\mu\text{g}$  DNA. In the box-and-whisker plot, the box represents the upper and lower quartile values (25–75% of data values). The median is represented by the midline. The whiskers extend to the 10th and 90th percentile of the data. Data were log transformed and statistical analyses displayed represent significant differences in vg values across dose groups or collection timepoints.  $P$ -values are adjusted for false-discovery rates using the Benjamin–Hochberg procedure to adjust for multiplicity in this mixed-model comparison. \* $p < 0.05$ , \*\* $p < 0.01$ , \*\*\* $p < 0.001$ , \*\*\*\* $p < 0.0001$ .

impact on SP-101 vg biodistribution (Fig. 2B–E), dosing with doxorubicin HCl had a large impact on *hCFTR* $\Delta R$  mRNA expression. In the absence of doxorubicin HCl, despite the higher dose of SP-101 (group I), *hCFTR* $\Delta R$  mRNA expression trended lower than a lower dose of SP-101 followed by doxorubicin HCl (group II) in all regions except for the nasal turbinates. The high dose of SP-101 followed by doxorubicin HCl (group III) demonstrated a significant 23-fold and 25-fold higher *hCFTR* $\Delta R$  mRNA expression in comparison to high dose SP-101 only (group I), based on median values, and reached the

median levels of endogenous *fCFTR* mRNA in lung and bronchus tissues, respectively. The median *hCFTR* $\Delta R$  mRNA levels in lung tissue samples were highest and, in agreement with SP-101 biodistribution, expression was lowest in tracheal samples.

To understand the durability of *hCFTR* $\Delta R$  mRNA expression in ferrets following a single dose of SP-101, or SP-101 followed by doxorubicin, tissue samples were evaluated 13 weeks post-dose in groups I, II, and III (Fig. 3). In contrast to the approximate 3-log decline of SP-101 vg at this time point, no significant decrease in median *hCFTR* $\Delta R$



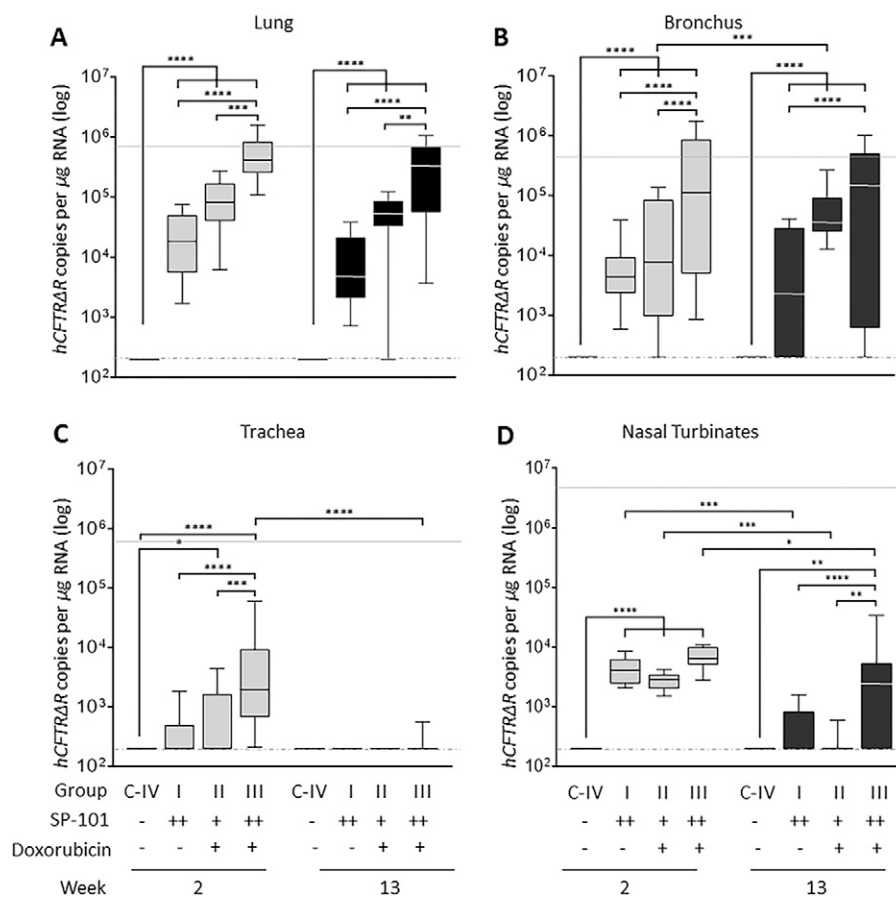


**Figure 3.** SP-101-mediated *hCFTRΔR* mRNA expression increases with increasing SP-101 dose and doxorubicin administration. Target tissues were collected from groups IV-C and I-III, 2- and 13-weeks post-dose, and evaluated for *hCFTRΔR* mRNA by RT-qPCR in (A) lung, (B) bronchus, (C) trachea ( $n = 14\text{--}24$  samples per group for the 3 tissue types) or (D) nasal turbinate tissue ( $n = 7\text{--}12$  samples per group). SP-101 ++ represents a high dose of SP-101 and + represents a low dose. For doxorubicin, + or — represents with or without doxorubicin (Dox), respectively. Endogenous ferret *CFTR* mRNA was evaluated in a multiplex reaction with *hCFTRΔR* mRNA and is plotted as median endogenous copies/ $\mu\text{g}$  RNA (light gray horizontal lines). Ct values were back calculated to plasmid standard curves and data are presented as *hCFTRΔR* copies/ $\mu\text{g}$  RNA. In the box-and-whisker plot, the boxes represent the upper and lower quartile values (25–75% of data values). The median is represented by the midline. The whiskers extend to the 10th and 90th percentile of the data. No *hCFTRΔR* mRNA was detected in control animals (group C-IV). The method lower limit of quantitation (LLOQ) is 200 copies per  $\mu\text{g}$  RNA. Samples with levels less than the LLOQ are plotted as 200 copies/ $\mu\text{g}$  RNA. Data were log transformed and statistical analyses displayed represent significant differences in mRNA copy values across dose groups or collection timepoints. P-values are adjusted for false-discovery rates using the Benjamin–Hochberg procedure to adjust for multiplicity in this mixed-model comparison. \* $p < 0.05$ , \*\* $p < 0.01$ , \*\*\* $p < 0.001$ , \*\*\*\* $p < 0.0001$ . CFTR, CF transmembrane conductance regulator.

mRNA copies was observed for any lung tissue dose group, bronchus (groups I and III) and trachea (groups I and II). This indicates the persistence of transcriptionally stable SP-101 vg that mediate *hCFTRΔR* mRNA expression in the lung and bronchus for at least 13-weeks post-dose (longest time-point investigated). Of potential importance, the levels of *hCFTRΔR* mRNA copies in the group receiving a high dose of SP-101 followed by doxorubicin HCl remained in the range of endogenous *fCFTR* mRNA (light gray line).

### Inhalation of SP-101 generates SP-101-neutralizing and-binding antibodies but a low cellular immune response

The immunogenicity of SP-101 in ferrets was evaluated by measuring anti-AAV2.5T (SP-101 capsid)

binding antibodies at serial time points post-dose in animals from groups I, II, and III (Fig. 4A). Pre-dose antibody titers for all animals were below the assay limit of detection. Post-dose samples from all animals revealed positive antibody titers emerging at the first post-dose time point (Week 2) that persisted through Week 13.

Neutralizing antibody titers to SP-101 were evaluated at the same time points in groups I, II, and III (Fig. 4B). No animal from any dose group tested positive for neutralizing antibodies pre-dose. Post-dose, all animals tested positive for SP-101 neutralizing antibodies from the first time point (Week 2) through the end of the evaluation period (Week 13). Empirically, there was an increase in neutralizing antibody titers from Week 2 to Week 6, but titers generally remained constant through the remainder of the evaluation period. Of interest, dosing with

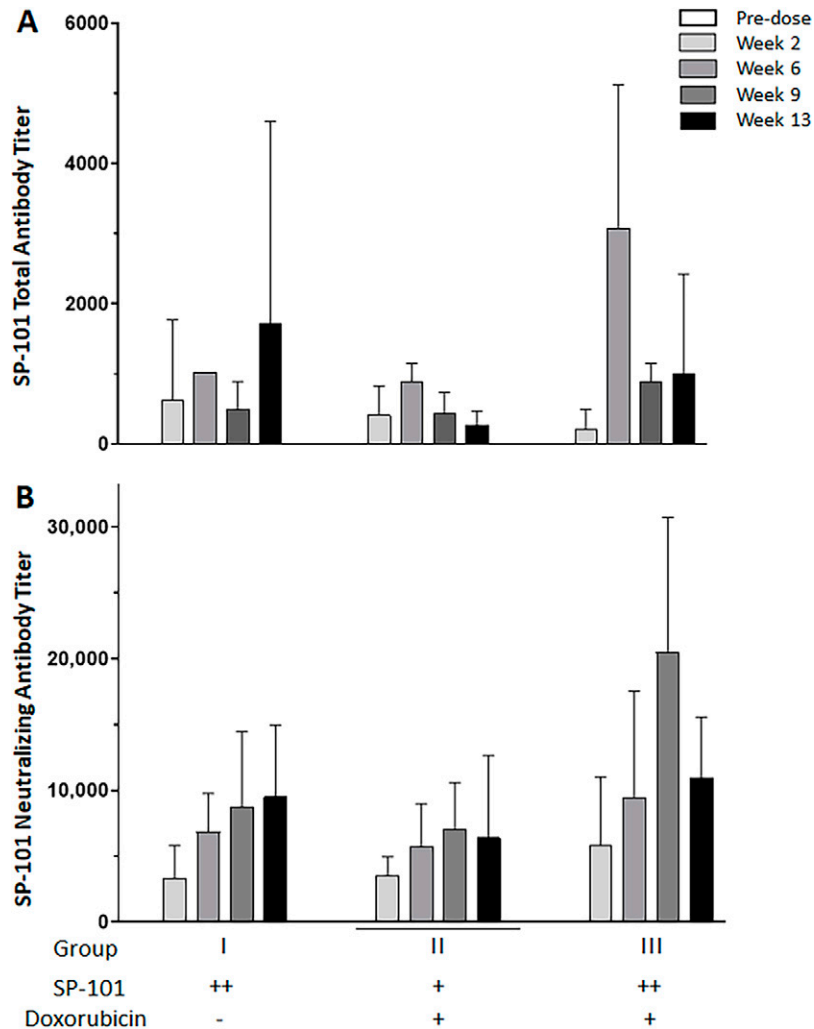


**Figure 4.** Inhalation of SP-101 generates SP-101-neutralizing and-binding antibodies. Blood samples were collected from ferrets pre-dose ( $n = 19-20$ ), dosed with SP-101 (high ++ or low +), with (+) or without (-) doxorubicin, in week 2 ( $n = 12$ ) or weeks 6, 9, and 13 ( $n = 3-8$ ) post-dose. **(A)** The generation of anti-AAV2.5T capsid-specific total antibodies in ferret serum were evaluated with a semi-quantitative, direct capture ELISA. **(B)** AAV2.5T neutralizing antibodies in ferret serum were evaluated with a cell-based transduction inhibition assay utilizing a HEK293 cell line and an AAV2.5T-LacZ reporter vector. Plotted values (titers) represent the dilution at which samples cross the assay cut point. For the binding antibody assay, the titer cut point was calculated as the 99<sup>th</sup> percentile of 30 drug-naïve ferret donors, tested in nine experimental runs by two analysts over four days. In the neutralizing antibody method, a sample is positive when the transduction signal is inhibited 50% compared to a naïve mouse serum control. Error bars represent group means  $\pm$  standard deviation. AAV2.5T, adeno-associated virus gene therapy vector.

doxorubicin HCl did not appear to influence AAV2.5T binding or neutralizing antibody titers.

The development of a cytotoxic T-cell response against the SP-101 capsid (AAV2.5T) and hCFTR $\Delta$ R following SP-101 dosing was evaluated in groups C-IV (saline control), I, II, and III. PBMCs were isolated from whole blood collected at the time of euthanasia at either Week 2 or Week 13 post dose. The T-cell response was evaluated in an IFN- $\gamma$  ELISpot assay using 3 peptide pools to the SP-101 capsid (AAV2.5T) (Fig. 5A) or 5 peptide pools to hCFTR $\Delta$ R (Fig. 5B). No samples were collected or evaluated from group III at 13-weeks post dose. PMA + ION stimulated PBMCs (positive control) resulted in the formation of 6–60 SFU when plated at  $2.0E3$  cells/well and 77-values above the quantifiable range of the plate reader

when plated at  $2.0E4$  cells/well. In contrast, only some animals from group I (Week 2) or group II (Week 13) were nominally higher than the cut-off threshold of 55 spot forming units per  $1E6$  cells/well PBMCs for the AAV2.5T peptide pools ( $<200$  SFU/ $1E6$  cells) indicating little to no cellular response to the AAV2.5T capsid. No PBMC samples from any group at either time point tested above the positive cut-off for the hCFTR $\Delta$ R peptide pools indicating a lack of cellular response despite expression of a foreign human CFTR $\Delta$ R protein.

#### SP-101 biodistribution and hCFTR $\Delta$ R mRNA expression is similar in CF and WT ferrets

The mucus or other structural changes found in the lungs of pwCF is thought to pose a barrier for gene therapy. To

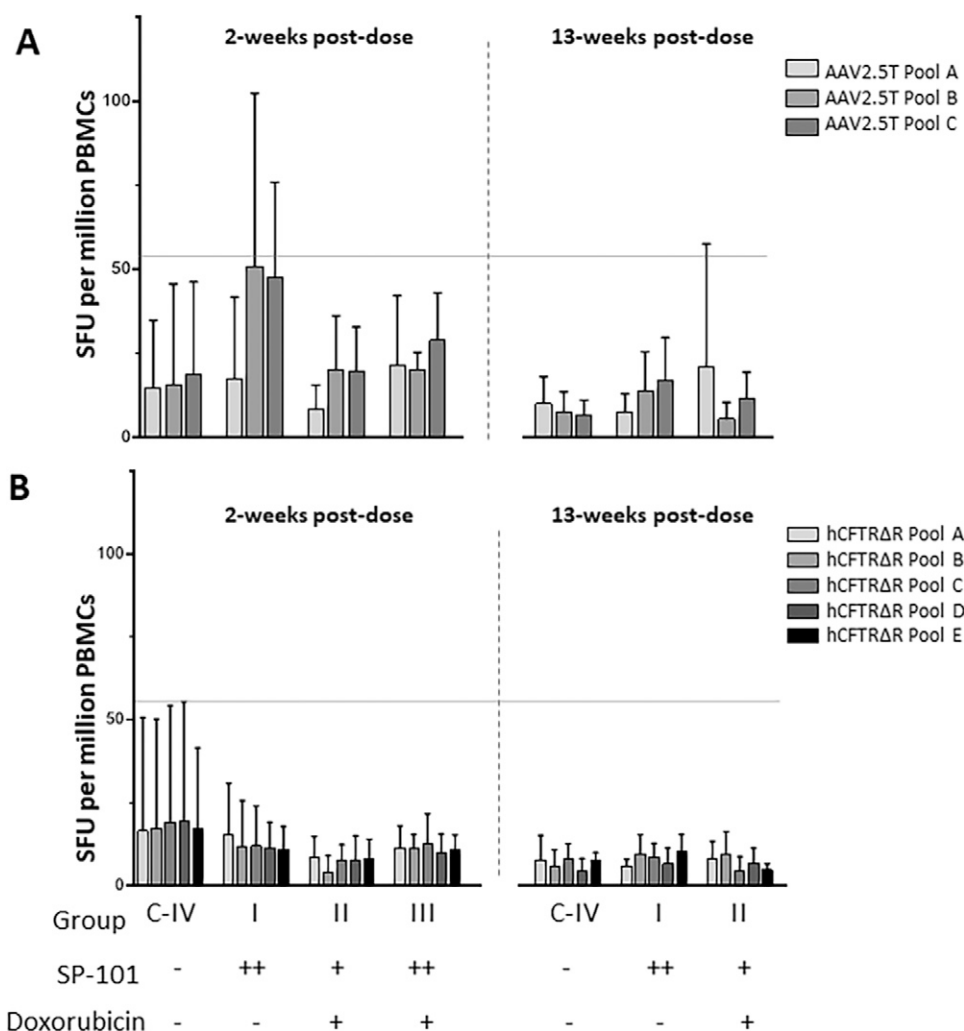


**Figure 5.** Low T-cell responses observed against the SP-101 capsid (AAV2.5T) and no response against *hCFTRΔR*. IFN- $\gamma$  ELISpot responses against (A) AAV2.5T capsid and (B) *hCFTRΔR* peptide library pools were evaluated in a total of 85 ferret PBMC samples with up to 12 ferrets or 8 ferrets in each dose group at weeks 2 or 13, respectively (note, no samples were obtained from group III at week 13). Ferrets were dosed with SP-101 (high ++ or low +), with (+) or without (–) doxorubicin. PBMC samples were also mock stimulated with DMSO (group C-IV, negative control) and PMA + ION stimulated PBMCs served as a positive control (not shown). The plotted values correspond to the mean SFU values per dose group/timepoint. Error bars represent group means  $\pm$  standard deviation. Gray horizontal lines represent cut-off threshold of 55 spot forming units per 1E6 cells/well. AAV2.5T, adeno-associated virus gene therapy vector; PMA + ION, phorbol myristate acetate plus ionomycin.

evaluate the potential impact, a comparison of the relative levels of SP-101 biodistribution (SP-101 vg copy counts) and expression (*hCFTRΔR* mRNA copy counts) between WT and CF (G551D CFTR genotype, off of ivacaftor for a minimum of 4 weeks) ferrets exposed to SP-101 via inhalation followed by doxorubicin via inhalation was evaluated on Week 2 post-dose as outlined in Figure 6A. The SP-101 lung deposited dose in CF ferrets (group VI: 2.6E11 vg/g) was determined to be 2-fold higher compared to WT (group V: 1.3E11 vg/g). The doxorubicin lung deposited dose level was 9  $\mu$ g/g in both groups. Comparable levels of SP-101 vector genomes were observed between WT and CF ferrets for each of the 3 tissue regions evaluated (Fig. 6B), with a trend for lower SP-101 copy counts in tracheal tissue versus lung and bronchus. The corresponding *hCFTRΔR* mRNA copy counts were also comparable between WT and CF

animals in the 3 tissue regions evaluated (Fig. 6C) with a similar trend for lower mRNA copy counts in tracheal tissue versus lung and bronchus. Endogenous levels of *fCFTR* mRNA were also determined for each tissue for each genotype. Median endogenous *fCFTR* mRNA values were comparable between the WT and CF animals for each tissue type; Lung 9.3E5 and 1.7E6, Bronchus 4.0E5 and 6.6E5 and Trachea 4.7E5 and 3.9E5 copies per  $\mu$ g total RNA for the WT and CF groups, respectively. While the number of animals in this study was small, taken together, these data suggest that the CF lung may not pose an additional barrier for SP-101 vg entry and *hCFTRΔR* mRNA expression.

To better understand the regionality of SP-101 biodistribution, tissues sections from animals in group V were investigated by *in-situ* hybridization (ISH). Sections were counterstained with H&E. Representative images of SP-101

*hCFTR* $\Delta R$  vg from one animal are shown in Figure 6D. The location of SP-101 vector genomes in these tissues are shown by the brown punctate dots (sense probe). Widespread distribution of SP-101 was observed with staining visible at both the apical surface of airways (bronchial region), as well as in the basal layer and within the alveolar regions (alveolar region). The specificity of the sense probe for DNA was confirmed by the absence of signal in the complementary images of slides pretreated with DNase prior to sense-probe addition.

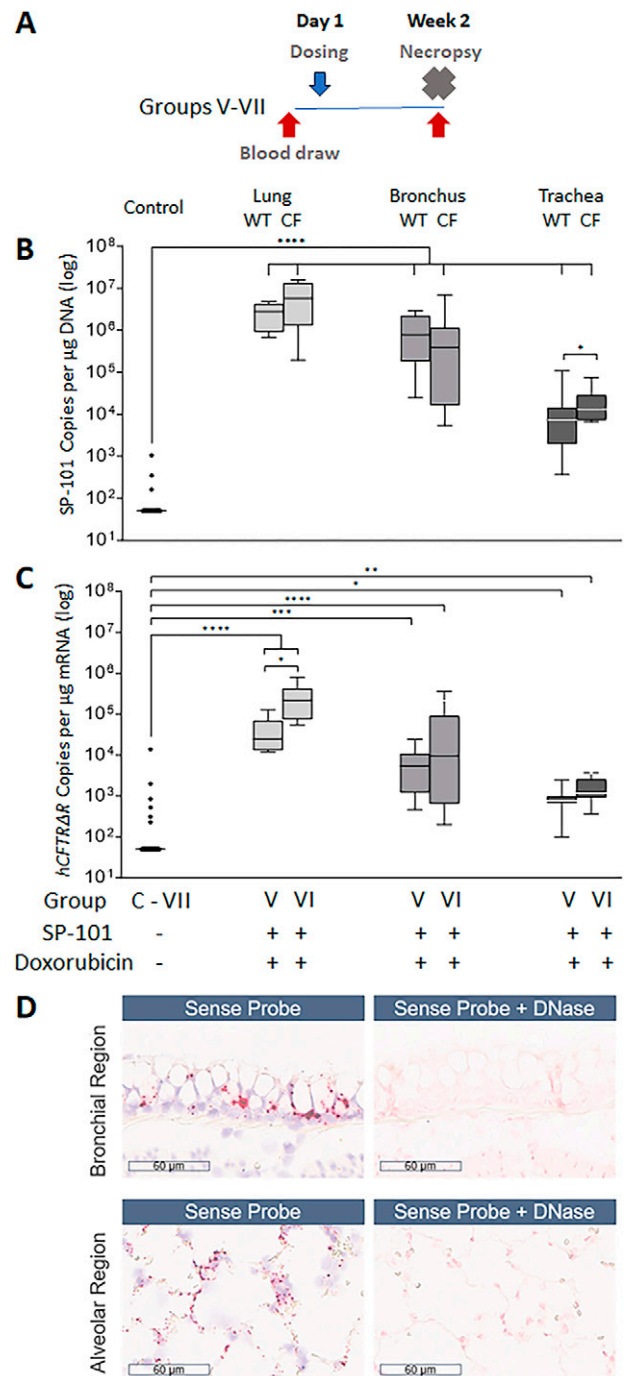
## DISCUSSION

The biodistribution, *hCFTR* $\Delta R$  mRNA expression, and immunogenicity after nebulized delivery of SP-101 alone, or SP-101 followed by inhaled doxorubicin HCl, was investigated in WT and CF ferrets. Biodistribution demonstrated both a dose response and regional differences that were closely reflected in the mRNA expression profile. However, in contrast to biodistribution, which was not altered by doxorubicin HCl, the number of *hCFTR* $\Delta R$  mRNA copies were significantly increased by doxorubicin HCl and reached similar levels to endogenous *fCFTR* mRNA. The positive impact of doxorubicin HCl on mRNA expression is consistent with both *in vitro* and *in vivo* literature showing that doxorubicin HCl can improve the gene expression resulting from many AAV serotypes.<sup>28–34</sup> As expected, based on other studies using the SP-101 capsid (AAV2.5T)<sup>31,32</sup> and other AAV serotypes,<sup>45,46</sup> nebulized delivery of SP-101 generated binding and neutralizing Ab responses but little cellular response to the capsid. No cellular response was detected for *hCFTR* $\Delta R$  despite administration to a ferret model. Importantly, SP-101 biodistribution and *hCFTR* $\Delta R$  mRNA expression was similar in a study that compared CF and WT ferrets.

**Figure 6.** SP-101 vg and *hCFTR* $\Delta R$  mRNA levels are similar between wild-type (WT) and CF ferrets. **(A)** Schematic of the study and sampling timeline. Target tissues were collected from either WT (group V) or CF (group VI) ferrets 2-weeks post-dose and evaluated for **(B)** SP-101 vector genomes and **(C)** *hCFTR* $\Delta R$  mRNA by qPCR and RT-qPCR, respectively. A total of 3 (WT) or 4 (CF) ferrets were dosed with SP-101 followed by doxorubicin, and 2–4 tissue samples were evaluated per region per animal. Ct values were back-calculated to a plasmid standard curve and data are presented as SP-101 copies/ $\mu$ g DNA or *hCFTR* $\Delta R$  copies/ $\mu$ g RNA. In the box-and-whisker plots, the box represents the upper and lower quartile values (25–75% of data values). The median is represented by the midline. The whiskers extend to the 10th and 90th percentile of the data. The lower limits of quantitation (LLOQ) are 50 copies per  $\mu$ g DNA or 200 copies per  $\mu$ g RNA. Samples with levels less than the LLOQ are plotted as 50 or 200 copies per  $\mu$ g/DNA or RNA, respectively. Data were log transformed and statistical analyses displayed represent significant differences across dose groups. P-values are adjusted for false-discovery rates using the Benjamini–Hochberg procedure to adjust for multiplicity in this mixed-model comparison. \* $p < 0.05$ , \*\* $p < 0.01$ , \*\*\* $p < 0.001$ , \*\*\*\* $p < 0.0001$ . **(D)** A representative *in situ* hybridization (ISH) image from group V. The scale bar represents 60  $\mu$ m. CF, cystic fibrosis.

The capsid for SP-101, AAV2.5T, was identified through directed evolution on primary human airway epithelia.<sup>20</sup> While initial tropism studies demonstrated little to no tropism for mouse (unpublished data) or pig airway epithelia,<sup>30</sup> AAV2.5T tropism was more recently demonstrated for the ferret airway *in vitro* and *in vivo*.<sup>31,32,47</sup> Since the level of tropism observed in ferret airway epithelia is similar to that in human airway epithelia *in vitro*, this created a pathway for development of SP-101.

As expected, the biodistribution of inhaled SP-101 in ferrets correlated with SP-101 deposited dose, with



groups I and III demonstrating higher SP-101 vg copy counts on Week 2 than the corresponding level observed in group II within each of the 4 tissue regions evaluated. The inclusion of doxorubicin HCl exposure for group III had no impact on the SP-101 vg copy counts observed 2-weeks post-dose, which is in agreement with *in vitro* CF HAE studies (reference companion *in vitro* paper). Although at 13-weeks post-dose SP-101 vg had declined roughly 3-log from 2-week levels, indicating that much of the initial dose had been cleared, significant levels persisted in lung and bronchus which is in agreement with durable *hCFTRΔR* mRNA expression. In general, the SP-101 vg copy counts observed in lung and bronchus tissues were higher than those observed in tracheal, nasal turbinate or non-respiratory tissue samples for each dose group. Future work is required to determine whether the regional differences in biodistribution are related to deposition upon nebulization, a difference in AAV2.5T receptor abundance or some other physiological parameter such as cellular composition.

SP-101-mediated *hCFTRΔR* mRNA expression was clearly apparent in all SP-101 dose groups 2-weeks and 13-weeks post-dose. Consistent with the SP-101 biodistribution, higher levels of *hCFTRΔR* mRNA expression were observed in lung and bronchial tissue, relative to tracheal or nasal turbinate. SP-101 alone was able to mediate *hCFTRΔR* mRNA expression (group I). However, similar to *in vitro* CF HAE studies, SP-101 followed by doxorubicin (group III) increased *hCFTRΔR* mRNA expression by 23-fold in the lung and 25-fold in the bronchus when compared to SP-101 alone, reaching levels of endogenous *fCFTR* mRNA that are more likely to have pharmacological relevance in the clinic. Since AAV2.5T was identified for its superior tropism to the cells of the human conducting airway, clinical trials in pwCF are required to understand the relevance of the expression levels observed in ferrets. Despite the typical use of doxorubicin HCl as a chemotherapeutic treatment, the addition of doxorubicin to increase AAV-mediated transgene expression, and subsequently functional transgene activity, has been considered for other AAV-based gene therapy programs.<sup>28-34</sup> While the existing approved clinical indications for doxorubicin require repeat IV dose administrations, the proposed use of doxorubicin as an augmenter of SP-101 gene therapy is limited to a single inhaled administration of a significantly lower dose than those used IV. Whether additional inhaled administrations of doxorubicin alone, subsequent to SP-101 administration, are able to further boost transgene expression requires additional studies.

The durability of expression is an important consideration for any gene therapy. In this study, no significant difference in SP-101-mediated *hCFTRΔR* mRNA expression was observed between weeks 2 and 13 with similar mRNA expression levels in both lung tissue and bronchus samples.

The turnover rate for airway cells in the lungs of people with or without CF remains a matter of debate. The half-life of a ciliated cell is estimated to be approximately 6 months and 17 months in the mouse trachea or lung, respectively.<sup>48</sup> Multiple AAV studies have shown durable gene expression for more than 5 to 9 months in the airways of mice, rabbits, and non-human primates.<sup>48-55</sup> Moreover, recent work in ferrets has demonstrated persistent ferret *CFTRΔR* mRNA expression 5 months after administration to WT ferrets.<sup>47</sup> While additional studies in animal models may lead to a better understanding of the duration of expression and mechanisms that may alter durability, stability data in humans is required to fully understand the durability of AAV-mediated lung gene therapy, particularly in pwCF. While the turnover of cells in the lung may be higher than those of the CNS, muscle, or eye, it is possible that lung-based expression in humans may ultimately be similar to other approved gene therapies which, to our knowledge, continue to yield expression many years after administration.<sup>45</sup>

One of the major factors that could negatively impact durability, as well as re-administration, is the immune response. Consistent with the data for other AAVs studied both in animal models and human clinical trials,<sup>45,46</sup> a single administration of SP-101 generated neutralizing and binding anti-capsid antibodies and a low capsid T-cell response. Doxorubicin did not appear to alter the immune response suggesting that the Ab response was likely due to acute exposure to the capsid rather than intracellular capsid trafficking or processing. We have previously shown that an acute immune response impairs vector re-administration in ferrets and that immunosuppression can reverse the impairment.<sup>31,32</sup> However, as expected, the neutralizing AAV2.5T Ab response in ferrets increased with AAV2.5T re-administration independent of concomitant immunosuppression.<sup>32</sup> In the absence of immunosuppression, a five-month interval between the first and repeat administration was sufficient to reduce systemic and bronchial lavage fluid IgG, IgA and IgM levels and allow successful AAV2.5T re-administration in ferrets.<sup>47</sup> These data indicate that the anti-SP-101 immune responses can be overcome without immunosuppression provided sufficient time has passed to allow for re-administration.

The generation or activation of a T-cell response to any CFTR gene therapy, including AAV-mediated *hCFTRΔR* expression, is a potential concern, particularly in pwCF carrying Class I mutations (null mutations). Calcedo et al. found that pre-existing CFTR-specific T-cells were present in 5–11.5% of subjects with CF.<sup>44</sup> While the clinical consequences of AAV gene therapy in this subset of subjects is unclear, particularly considering almost 12% of non-CF subjects also had CFTR-specific T-cells, the magnitude of activation of CFTR-specific T cells is an important parameter to monitor. In the present study, no cellular response

was observed for hCFTR $\Delta$ R despite having only 91.9% identity with fCFTR.<sup>56</sup> One limitation to this study is that the ferrets evaluated were WT. Although CFTR-specific T-cell responses have been detected in other gene transfer studies conducted in WT animal models,<sup>46,57</sup> potentially CFTR knockout animals may represent a more accurate model to predict T-cell responses in pwCF carrying Class I (null) CFTR mutations.

In order to understand whether SP-101 can mediate gene expression in the CF lung, a comparison of SP-101 vector genome distribution in lung, bronchus or trachea was performed in CF ferrets in comparison to WT ferrets. In this study, the dose of SP-101 in CF ferrets was twice that of WT animals while the dose of doxorubicin was identical between the 2 groups. No significant difference in SP-101 biodistribution was observed between CF and WT ferrets. However, hCFTR $\Delta$ R mRNA expression was significantly increased in CF ferret lung over WT animals ( $p = 0.025$ ), but not bronchus ( $p = 0.301$ ) or trachea ( $p = 0.528$ ), 2-weeks post-dose. Taken together, these data suggest that the lungs of CF ferrets, in this study, did not pose an additional barrier to SP-101-mediated gene expression. Unfortunately, at the time of this study, no functional endpoints for CFTR were available in CF ferret lung or trachea *in vivo*. Any future study would incorporate an endpoint such as the recently developed mucociliary clearance assay.<sup>58</sup> However, as a proof of concept, directed AAV evolution in pigs yielded AAV2H22, a capsid with high tropism to the pig airway epithelium.<sup>30</sup> AAV2H22 carrying the hCFTR $\Delta$ R transgene driven by a shortened CMV promoter, in combination with doxorubicin, successfully restored chloride current and corrected multiple CF-related phenotypes in the airways of neonatal gut-corrected CFTR-null pigs, thereby validating the approach of using an AAV vector carrying a hCFTR $\Delta$ R payload to correct CFTR dysfunction in the respiratory system *in vivo*.

ISH using a sense probe that detects SP-101 vg, but not hCFTR $\Delta$ R mRNA, demonstrated widespread presence of SP-101 genomes 2 weeks post-dose, in both bronchial and alveolar regions (group V). Specificity of the sense probe was demonstrated via DNase treatment, which also removed the majority of the staining for the nuclei resulting in a lighter background. ISH for AAV-mediated transgene mRNA expression is technically challenging because AAV virions contain both positive and negative single-stranded DNA genomes that can bind anti-sense and sense probes, respectively. Moreover, the AAV vg is abundant throughout the cell cytoplasm and nucleus meaning that subcellular localization cannot be used to distinguish between vg and mRNA. Additionally, the small size of the vg makes it a challenge to remove using most standard DNase

applications. Significant additional optimization is required to confidently detect hCFTR $\Delta$ R mRNA by ISH in these tissues and may not be possible given that the SP-101 vg levels are  $\sim 10$ -fold higher than mRNA based on a  $\mu\text{g}$  DNA to  $\mu\text{g}$  RNA comparison (Figs. 2, 3, 6). Despite these caveats, the detection of SP-101 vg is robust and provides evidence for its lung tropism *in vivo*.

Currently, multiple clinical trials investigating various types of genetic therapies for CF are ongoing, including AAV (NCT05248230), herpes simplex virus-1 (NCT05504837/NCT05095246), anti-sense oligonucleotides (NCT06429176) and mRNA (NCT05668741/NCT05712538/NCT06237335). While these trials provide several opportunities for success, it is likely no one therapy will work for all pwCF, especially if there is a vector or drug-derived immune response or intolerance. Moreover, it is likely that re-administration will be required for airway-directed gene therapy. While the necessity for additional dose(s) of SP-101 with doxorubicin to maintain hCFTR $\Delta$ R activity levels will be determined once single dose clinical data are in-hand, the most direct way to circumvent a persistent anti-capsid Ab response to a viral vector is to use a different vector. Thus, multiple different genetic modalities are expected to be required to treat the remaining pwCF who do not benefit from modulator therapies. Overall, the data presented here are supportive of further development of inhaled SP-101 followed by inhaled doxorubicin HCl and warrants clinical investigation (NCT06526923).

## ACKNOWLEDGMENTS

The authors thank the Immunology Core of the Gene Therapy Program at the University of Pennsylvania for Neutralizing Antibody and ELISpot assay support, and the LBA team at KCAS Bioanalytical and Biomarker Services in Olathe, KS for method development and validation of the Total Antibody assay, and Lovelace Biomedical Research Institute for their support of this work. The authors would also like to thank Charles Gu and Stephanie Pasas-Farmer of Biodata Solutions for providing statistical analysis support. All work was funded by Spirovant Sciences, Inc.

## AUTHORS' CONTRIBUTIONS

K.J.D.A.E.: Conceptualization, Writing—Original Draft, Visualization, Supervision. M.D.S.: Conceptualization, Writing—Original Draft, Visualization, Supervision, Project Administration. L.F.: Methodology, Validation, Formal Analysis, Writing—Original Draft, Visualization, Project Administration. R.S.: Conceptualization, Writing—Review and Editing, Project Administration. S.L.: Formal Analysis, Investigation, Writing—Review and Editing, Visualization. M.M.: Formal Analysis,

Investigation, Writing—Review and Editing. P.K.L.N.: Investigation, Writing—Review and Editing, Visualization. M.G.: Formal Analysis, Writing—Review and Editing, Project Administration. M.P.L.: Formal Analysis, Writing—Review and Editing. E.Y.: Conceptualization, Supervision, Funding Acquisition. R.K.: Conceptualization, Writing—Review and Editing, Supervision, Funding Acquisition.

## AUTHOR DISCLOSURE

All authors were employees of Spirovant Sciences, Inc. when this work was conducted.

## FUNDING INFORMATION

All work was funded by Spirovant Sciences, Inc.

## DATA AVAILABILITY STATEMENT

Data available upon request.

## SUPPLEMENTARY MATERIAL

Supplementary Figure S1

## REFERENCES

- Choi SH, Engelhardt JF. Gene therapy for cystic fibrosis: Lessons learned and paths forward. *Mol Ther* 2021;29(2):428–430; doi: 10.1016/j.ymthe.2021.01.010
- De Boeck K. Cystic fibrosis in the year 2020: A disease with a new face. *Acta Paediatr* 2020; 109(5):893–899; doi: 10.1111/apa.15155
- Stoltz DA, Meyerholz DK, Welsh MJ. Origins of cystic fibrosis lung disease. *N Engl J Med* 2015; 372(4):351–362; doi: 10.1056/NEJMra1300109
- Ensinck MM, Carlon MS. One size does not fit all: The past, present and future of cystic fibrosis causal therapies. *Cells* 2022;11(12); doi: 10.3390/cells11121868
- Ridley K, Condren M. Elexacaftor-Tezacaftor-Ivacaftor: The first triple-combination cystic fibrosis transmembrane conductance regulator modulating therapy. *J Pediatr Pharmacol Ther* 2020;25(3):192–197; doi: 10.5863/1551-6776-25.3.192
- Tummler B. Post-approval studies with the CFTR modulators Elexacaftor-Tezacaftor-Ivacaftor. *Front Pharmacol* 2023;14:1158207; doi: 10.3389/fphar.2023.1158207
- Cooney AL, McCray PB, Jr, Sinn PL. Cystic fibrosis gene therapy: Looking back, looking forward. *Genes (Basel)* 2018;9(11); doi: 10.3390/genes9110538
- Griesenbach U, Pytel KM, Alton EW. Cystic fibrosis gene therapy in the UK and elsewhere. *Hum Gene Ther* 2015;26(5):266–275; doi: 10.1089/hum.2015.027
- Sui H, Xu X, Su Y, et al. Gene therapy for cystic fibrosis: Challenges and prospects. *Front Pharmacol* 2022;13:1015926; doi: 10.3389/fphar.2022.1015926
- Loring HS, ElMallah MK, Flotte TR. Development of rAAV2-CFTR: History of the first rAAV vector product to be used in humans. *Hum Gene Ther Methods* 2016;27(2):49–58; doi: 10.1089/hgtb.2015.150
- Flotte T, Carter B, Conrad C, et al. A phase I study of an adeno-associated virus-CFTR gene vector in adult CF patients with mild lung disease. *Hum Gene Ther* 1996;7(9):1145–1159; doi: 10.1089/hum.1996.7.9-1145
- Wagner JA, Messner AH, Moran ML, et al. Safety and biological efficacy of an adeno-associated virus vector-cystic fibrosis transmembrane regulator (AAV-CFTR) in the cystic fibrosis maxillary sinus. *Laryngoscope* 1999; 109(2 Pt 1):266–274; doi: 10.1097/00005537-199902000-00017
- Aitken ML, Moss RB, Waltz DA, et al. A phase I study of aerosolized administration of tgAAVCF to cystic fibrosis subjects with mild lung disease. *Hum Gene Ther* 2001;12(15):1907–1916; doi: 10.1089/104303401753153956
- Wagner JA, Nepomuceno IB, Messner AH, et al. A phase II, double-blind, randomized, placebo-controlled clinical trial of tgAAVCF using maxillary sinus delivery in patients with cystic fibrosis with antrostomies. *Hum Gene Ther* 2002;13(11): 1349–1359; doi: 10.1089/104303402760128577
- Flotte TR, Zeitlin PL, Reynolds TC, et al. Phase I trial of intranasal and endobronchial administration of a recombinant adeno-associated virus serotype 2 (rAAV2)-CFTR vector in adult cystic fibrosis patients: A two-part clinical study. *Hum Gene Ther* 2003;14(11):1079–1088; doi: 10.1089/104303403322124792
- Moss RB, Rodman D, Spencer LT, et al. Repeated adeno-associated virus serotype 2 aerosol-mediated cystic fibrosis transmembrane regulator gene transfer to the lungs of patients with cystic fibrosis: A multicenter, double-blind, placebo-controlled trial. *Chest* 2004;125(2): 509–521; doi: 10.1378/chest.125.2.509
- Moss RB, Milla C, Colombo J, et al. Repeated aerosolized AAV-CFTR for treatment of cystic fibrosis: A randomized placebo-controlled phase 2B trial. *Hum Gene Ther* 2007;18(8):726–732; doi: 10.1089/hum.2007.022
- Zabner J, Seiler M, Walters R, et al. Adeno-associated virus type 5 (AAV5) but not AAV2 binds to the apical surfaces of airway epithelia and facilitates gene transfer. *J Virol* 2000;74(8):3852–3858; doi: 10.1128/jvi.74.8.3852-3858.2000
- Siminger J, Muller C, Braag S, et al. Functional characterization of a recombinant adeno-associated virus 5-pseudotyped cystic fibrosis transmembrane conductance regulator vector. *Hum Gene Ther* 2004; 15(9):832–841; doi: 10.1089/hum.2004.15.832
- Excoffon KJ, Koerber JT, Dickey DD, et al. Directed evolution of adeno-associated virus to an infectious respiratory virus. *Proc Natl Acad Sci U S A* 2009;106(10):3865–3870; doi: 10.1073/pnas.0813365106
- Dickey DD, Excoffon KJ, Koerber JT, et al. Enhanced sialic acid-dependent endocytosis explains the increased efficiency of infection of airway epithelia by a novel adeno-associated virus. *J Virol* 2011;85(17):9023–9030; doi: 10.1128/JVI.05154-11
- Ostedgaard LS, Zabner J, Vermeer DW, et al. CFTR with a partially deleted R domain corrects the cystic fibrosis chloride transport defect in human airway epithelia in vitro and in mouse nasal mucosa in vivo. *Proc Natl Acad Sci U S A* 2002; 99(5):3093–3098; doi: 10.1073/pnas.261714599
- Ostedgaard LS, Rokhlina T, Karp PH, et al. A shortened adeno-associated virus expression cassette for CFTR gene transfer to cystic fibrosis airway epithelia. *Proc Natl Acad Sci U S A* 2005;102(8):2952–2957; doi: 10.1073/pnas.0409845102
- Ostedgaard LS, Meyerholz DK, Vermeer DW, et al. Cystic fibrosis transmembrane conductance regulator with a shortened R domain rescues the intestinal phenotype of CFTR<sup>-/-</sup> mice. *Proc Natl Acad Sci U S A* 2011;108(7): 2921–2926; doi: 10.1073/pnas.1019752108
- Yan Z, Sun X, Feng Z, et al. Optimization of recombinant adeno-associated virus-mediated expression for large transgenes, using a synthetic promoter and tandem array enhancers.

- Hum Gene Ther 2015;26(6):334–346; doi: 10.1089/hum.2015.001
26. Duan D, Yue Y, Yan Z, et al. Endosomal processing limits gene transfer to polarized airway epithelia by adeno-associated virus. *J Clin Invest* 2000;105(11):1573–1587; doi: 10.1172/JCI8317
  27. Duan D, Yue Y, Yan Z, et al. Polarity influences the efficiency of recombinant adeno-associated virus infection in differentiated airway epithelia. *Hum Gene Ther* 1998;9(18):2761–2776; doi: 10.1089/hum.1998.9.18-2761
  28. Yan Z, Zak R, Zhang Y, et al. Distinct classes of proteasome-modulating agents cooperatively augment recombinant adeno-associated virus type 2 and type 5-mediated transduction from the apical surfaces of human airway epithelia. *J Virol* 2004;78(6):2863–2874; doi: 10.1128/jvi.78.6.2863-2874.2004
  29. Zhang LN, Karp P, Gerard CJ, et al. Dual therapeutic utility of proteasome modulating agents for pharmaco-gene therapy of the cystic fibrosis airway. *Mol Ther* 2004;10(6):990–1002; doi: 10.1016/j.ymthe.2004.08.009
  30. Steines B, Dickey DD, Bergen J, et al. CFTR gene transfer with AAV improves early cystic fibrosis pig phenotypes. *JCI Insight* 2016;1(14):e88728; doi: 10.1172/jci.insight.88728
  31. Tang Y, Yan Z, Lin S, et al. Repeat dosing of AAV2.5T to ferret lungs elicits an antibody response that diminishes transduction in an age-dependent manner. *Mol Ther Methods Clin Dev* 2020;19:186–200; doi: 10.1016/j.omtm.2020.09.008
  32. Tang Y, Fakhari S, Huntemann ED, et al. Immunosuppression reduces rAAV2.5T neutralizing antibodies that limit efficacy following repeat dosing to ferret lungs. *Mol Ther Methods Clin Dev* 2023;29:70–80; doi: 10.1016/j.omtm.2023.02.015
  33. Cui S, Ganjawala TH, Abrams GW, et al. Effect of proteasome inhibitors on the AAV-mediated transduction efficiency in retinal bipolar cells. *Curr Gene Ther* 2020;19(6):404–412; doi: 10.2174/1566523220666200211111326
  34. Gong H, Yuan N, Shen Z, et al. Transduction catalysis: Doxorubicin amplifies rAAV-mediated gene expression in the cortex of higher-order vertebrates. *iScience* 2021;24(6):102685; doi: 10.1016/j.isci.2021.102685
  35. Yan Z, Sun X, Evans IA, et al. Postentry processing of recombinant adeno-associated virus type 1 and transduction of the ferret lung are altered by a factor in airway secretions. *Hum Gene Ther* 2013;24(9):786–796; doi: 10.1089/hum.2013.137
  36. Sun X, Sui H, Fisher JT, et al. Disease phenotype of a ferret CFTR-knockout model of cystic fibrosis. *J Clin Invest* 2010;120(9):3149–3160; doi: 10.1172/JCI43052
  37. Sun X, Yan Z, Yi Y, et al. Adeno-associated virus-targeted disruption of the CFTR gene in cloned ferrets. *J Clin Invest* 2008;118(4):1578–1583; doi: 10.1172/JCI34599
  38. Sun X, Olivier AK, Liang B, et al. Lung phenotype of juvenile and adult cystic fibrosis transmembrane conductance regulator-knockout ferrets. *Am J Respir Cell Mol Biol* 2014;50(3):502–512; doi: 10.1165/rcmb.2013-0261OC
  39. Keiser NW, Birket SE, Evans IA, et al. Defective innate immunity and hyperinflammation in newborn cystic fibrosis transmembrane conductance regulator-knockout ferret lungs. *Am J Respir Cell Mol Biol* 2015;52(6):683–694; doi: 10.1165/rcmb.2014-0250OC
  40. Sun X, Yi Y, Yan Z, et al. In utero and postnatal VX-770 administration rescues multiorgan disease in a ferret model of cystic fibrosis. *Sci Transl Med* 2019;11(485); doi: 10.1126/scitranslmed.aau7531
  41. Ding W, Zhang LN, Yeaman C, et al. rAAV2 traffics through both the late and the recycling endosomes in a dose-dependent fashion. *Mol Ther* 2006;13(4):671–682; doi: 10.1016/j.ymthe.2005.12.002
  42. Calcedo R, Vandenbergh LH, Gao G, et al. Worldwide epidemiology of neutralizing antibodies to adeno-associated viruses. *J Infect Dis* 2009;199(3):381–390; doi: 10.1086/595830
  43. Calcedo R, Chichester JA, Wilson JM. Assessment of humoral, innate, and T-Cell immune responses to adeno-associated virus vectors. *Hum Gene Ther Methods* 2018;29(2):86–95; doi: 10.1089/hgtb.2018.038
  44. Calcedo R, Griesenbach U, Dorgan DJ, et al. Self-reactive CFTR T cells in humans: Implications for gene therapy. *Hum Gene Ther Clin Dev* 2013;24(3):108–115; doi: 10.1089/humc.2012.249
  45. Mendell JR, Al-Zaidy SA, Rodino-Klapac LR, et al. Current clinical applications of *In Vivo* gene therapy with AAVs. *Mol Ther* 2021;29(2):464–488; doi: 10.1016/j.ymthe.2020.12.007
  46. Muhuri M, Maeda Y, Ma H, et al. Overcoming innate immune barriers that impede AAV gene therapy vectors. *J Clin Invest* 2021;131(1); doi: 10.1172/JCI143780
  47. Tang Y, Ebadi M, Lei J, et al. Durable transgene expression and efficient re-administration after rAAV2.5T-mediated fCFTRDeltaR gene delivery to adult ferret lungs. *Mol Ther Methods Clin Dev* 2024;32(2):101244; doi: 10.1016/j.omtm.2024.101244
  48. Rawlins EL, Hogan BL. Ciliated epithelial cell lifespan in the mouse trachea and lung. *Am J Physiol Lung Cell Mol Physiol* 2008;295(1):L231–L234; doi: 10.1152/ajplung.90209.2008
  49. Halbert CL, Standaert TA, Wilson CB, et al. Successful readministration of adeno-associated virus vectors to the mouse lung requires transient immunosuppression during the initial exposure. *J Virol* 1998;72(12):9795–9805; doi: 10.1128/JVI.72.12.9795-9805.1998
  50. Halbert CL, Rutledge EA, Allen JM, et al. Repeat transduction in the mouse lung by using adeno-associated virus vectors with different serotypes. *J Virol* 2000;74(3):1524–1532; doi: 10.1128/jvi.74.3.1524-1532.2000
  51. Joyeux L, Danzer E, Limberis MP, et al. In utero lung gene transfer using adeno-associated viral and lentiviral vectors in mice. *Hum Gene Ther Methods* 2014;25(3):197–205; doi: 10.1089/hgtb.2013.143
  52. Kang MH, van Lieshout LP, Xu L, et al. A lung tropic AAV vector improves survival in a mouse model of surfactant B deficiency. *Nat Commun* 2020;11(1):3929; doi: 10.1038/s41467-020-17577-8
  53. Flotte TR, Afione SA, Zeitlin PL. Adeno-associated virus vector gene expression occurs in nondividing cells in the absence of vector DNA integration. *Am J Respir Cell Mol Biol* 1994;11(5):517–521; doi: 10.1165/ajrcmb.11.5.7946381
  54. Conrad CK, Allen SS, Afione SA, et al. Safety of single-dose administration of an adeno-associated virus (AAV)-CFTR vector in the primate lung. *Gene Ther* 1996;3(8):658–668.
  55. Afione SA, Conrad CK, Kearns WG, et al. In vivo model of adeno-associated virus vector persistence and rescue. *J Virol* 1996;70(5):3235–3241; doi: 10.1128/JVI.70.5.3235-3241.1996
  56. Fisher JT, Liu X, Yan Z, et al. Comparative processing and function of human and ferret cystic fibrosis transmembrane conductance regulator. *J Biol Chem* 2012;287(26):21673–21685; doi: 10.1074/jbc.M111.336537
  57. Limberis MP, Figueredo J, Calcedo R, et al. Activation of CFTR-specific T Cells in cystic fibrosis mice following gene transfer. *Mol Ther* 2007;15(9):1694–1700; doi: 10.1038/sj.mt.6300210
  58. Yuan F, Gasser GN, Lemire E, et al. Transgenic ferret models define pulmonary ionocyte diversity and function. *Nature* 2023;621(7980):857–867; doi: 10.1038/s41586-023-06549-9

Received for publication April 24, 2024;  
accepted after revision July 15, 2024.

Published online: August 19, 2024.